Electronic Supplementary Information

A Metal-Free, High Nitrogen-Doped Nanoporous Graphitic Carbon Catalyst for an Effective Aerobic HMF-to-FDCA Conversion

Chi Van Nguyen,[a] Yu-Te Liao,[a] Ting-Cih Kang,[a] Jeffrey E. Chen,[a] Takuya Yoshikawa,[b] Yuta Nakasaka,[b] Takao Masuda,[b] and Kevin C.-W. Wu[a]*

[a] Department of Chemical Engineering, National Taiwan University, No. 1, Sec. 4, Roosevelt Road, Taipei 10617 (Taiwan), Fax :(+ 886) 2-2362-304

[b] Division of Applied Chemistry, Hokkaido University, Kita-13 Nishi-8, Kita-ku, Sapporo, Hokkaido 060-8628, Japan

Email: kevinwu@ntu.edu.tw

Experimental section

Chemicals

5-hydroxymethylfurfural (HMF; 99%), 2,5-furandicarboxylic acid (FDCA; 99%) and 5-hydroxymethyl-2-furancarboxylic acid (HMFCA; 99%), 5-formyl-2-furancarboxylic acid (FFCA), 2,5-diformyfuran (DFF; 97%), succinic acid (99%), levulinic acid (97%), sodium hydroxide (98%), potassium hydroxide (98%), potassium carbonate (99%), sodium carbonate (99%), potassium phosphate tribasic (99%), sodium phosphate (96%), potassium bicarbonate (99%) sodium bicarbonate (99%), methanol anhydrous (99.8%), zinc nitrate hexahydrate (98%) and 2-methylimidazole (99%) were purchased from Sigma-aldrich or Acros Company and were used without further purification.

Synthesis of nitrogen-doped nanoporous carbon (NNC) materials

Nitrogen-doped porous carbons were synthesized analogous to the previous literature with slight modifications.[1] Typically, 2-methylimidazole (4.2 g, 0.088 mol) and

polyvinylpyrrolidone (K-30, 12 g) was dissolved into methanol (150 mL). $Zn(NO_3)_2 \cdot 6H_2O$ (4.4 g, 0.023 mol) was dissolved in methanol (150 mL), and the mixture was added into the 2-methylimidazole solution dropwise by using syringe with stiring for 30 min. After 12h, the white powders were centrifuged and washed carefully with methanol. The dry powder was activated at 150 ^{o}C for 5 h in vacuum to remove 2-methylimidazole residues. The activated powders (ZIF-8) were carbonized directly under nitrogen atmosphere at various temperatures (i.e., From 600 to 900 °C) for 8h with a heating rate of 5 °C·min^{-1}. The samples were named to be NNC-*x*, where *x* means the calcination temperature. After carbonization, the residual zinc component was removed by using concentrated HCl (36.5%). Finally, the resulting samples was washed several times with dionized water and methanol, activated at 150 °C for 5h prior to catalytic reactions.

Characterization

Powder X-ray diffraction (XRD) patterns were recored using a Cu Kα radiation source on a Rigaku-Ultima IV instrument. The morphology of the the synthesized samples was observed with scanning electron microscopy (SEM, Nova^{TM} NanoSEM 230). Nitrogen adsorption/desorption measurements were conducted using a micromeritics ASAP 2020 for porous properties including specific surface area and pore size. The chemical state of nitrogen (i.e. N-1s) was performed on an X-ray photoelectron spectroscopy (XPS, Thermo Scientific, Theta Probe). The chemical composition of samples (i.e., carbon, nitrogen, hydrogen, and zinc) was analyzed with Elemental Vario EL cube (for NCSH, German) and plasma mass spectrometry (ICP-MS).

Catalytic reaction

The aerobic oxidation of HMF to FDCA was carried out in a round bottom flask fitted with a reflux condenser. Typically, a mixture of HMF (0.63 mmol;), catalysts (0.2 g) and K_2CO_3 (0.189 mmol) was added into a 25 ml three-neck flask containing 10 ml of water. The oxygen gas was purged into the mixture with a flow rate 100 mL·min^{-1} oxygen gas at 1 atm. The reaction mixture was heated at 80 ^{o}C for 48h under a magnetically stirred. After 48h, the product was cooled to room temperature and diluted into 25 ml with deionized water. The solution was filtered with a syringe filter (0.22 μm pore size) for HPLC analysis.

Analysis of products

An external standard calibration curve was utilized to calculate concentration of HMF and all products that were quantifed with HPLC beforehand (an ICE-Coregel 87H3 column; operation at 35 °C). The mobile phase was 8 mM sulfuric acid equeous solution at a flow rate of 0.6 mL·min^{-1}. The conversion *X* and products yield *Y* are calculated by the following formula, and where [] is concentration.

$$\mathrm{X}\ (mol\%) = \frac{[HMF]_{initial} - [HMF]_{after\ reaction}}{[HMF]_{initial}}$$

The yield of products in the solution is calculated to be:

$$Y_i\ (mol\%) = \frac{([product]_i)_{formed}}{[HMF]_{initial}}$$

Results

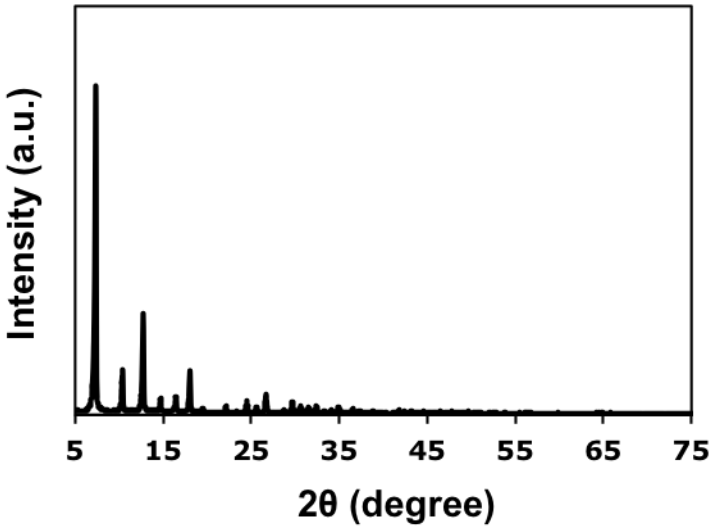

Figure S1: The XRD pattern of the synthesized ZIF-8 sample.

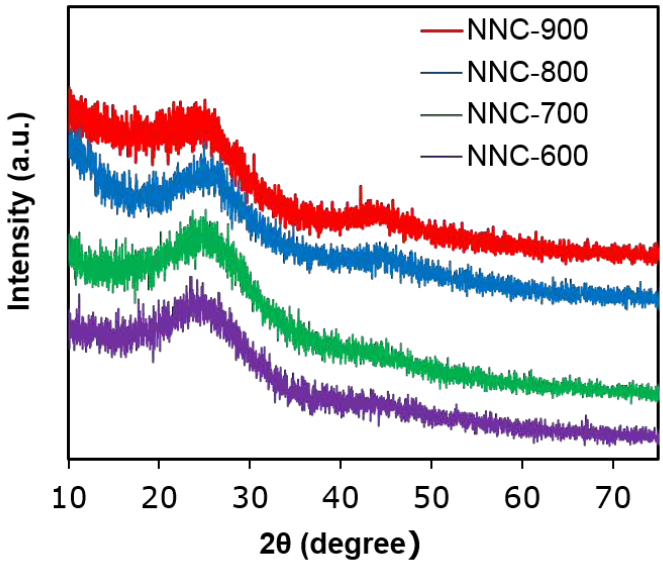

Figure S2: XRD patterns of ZIF-8-derived NNC-X materials at different pyrolysis temperatures; X refer to carbonization temperatures.

Table S1: Composition of ZIF-8-derived N-doped carbon particles

Samples	Elemental analysis (wt%)				N_{1s} (%)[a]		
	N	C	H	Zn	N-6	N-5	N-Q
NNC-900	15.32	64.51	1.44	8.6	47.13	27.6	25.27
NNC-800	21.64	58.51	1.60	6.2	58.57	25.17	16.26
NNC-700	27.71	54.93	1.68	3.5	58.52	32.78	8.7
NNC-600	29.45	53.43	3.24	3.3	89.3	6.16	4.5
Spent NNC-900	14.29	63.45	1.26	-	56.63	25.48	20.89

[a] From XPS spectra

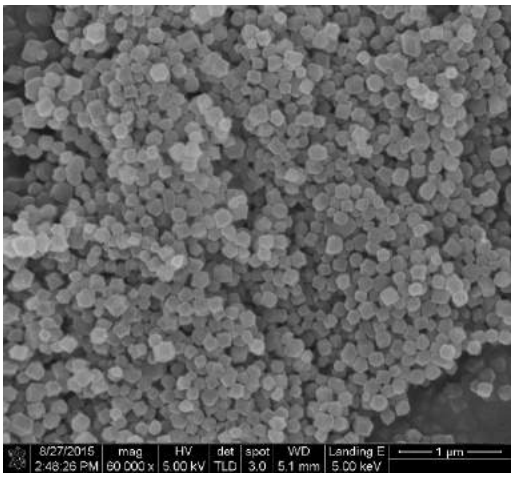

Figure S3: The SEM image of the synthesized ZIF-8 material.

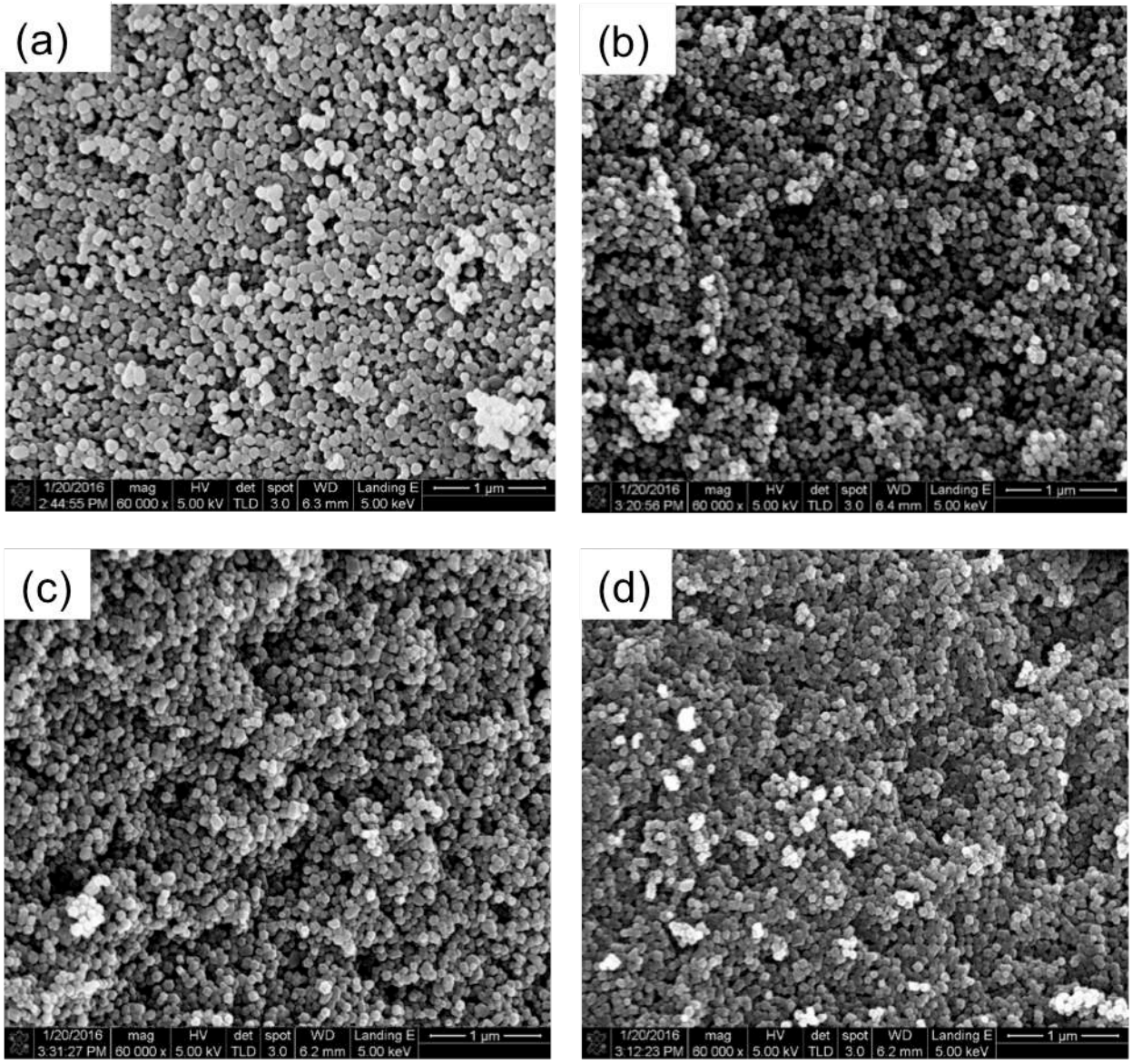

Figure S4: SEM images of the ZIF-8-derived NNC-X materials; X refers to carbonization temperatures. (a) 600, (b) 700, (c) 800, (d) 900 ^{o}C.

Table S2: Pore characteristic of ZIF-8 and NCC-X samples

Samples	Specific surface area (m^2/g) [a]	Pore size (nm) [b]	Micropore volume (cm^3/g) [c]	Mesopore volume (cm^3/g) [d]
ZIF-8	1428	1.2, 1.5	0.17	0.85
NNC-900	813	0.59	0.35	0.76
NNC-800	833	0.59	0.29	0.65
NNC-700	795	0.59	0.35	0.58
NNC-600	601	0.59	0.26	0.65
Spent NNC-900	110	0.59	0.02	0.42

[a]: Specific surface area is calculated with BET theory.

[b]: Pore size is calculated with NLDFT model assuming slit carbon pores.

[c]: Micropore volume is calculated with t-plot value.

[d]: Mesopore volume is the difference of single pore volume and t-plot micropore volume

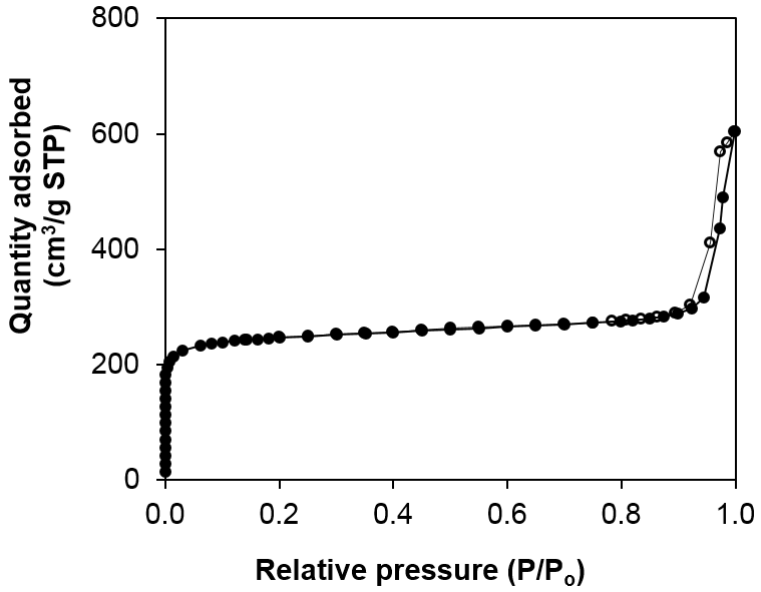

Figure S5: Nitrogen adsorption/desorption isotherm curve of the synthesized ZIF-8 material.

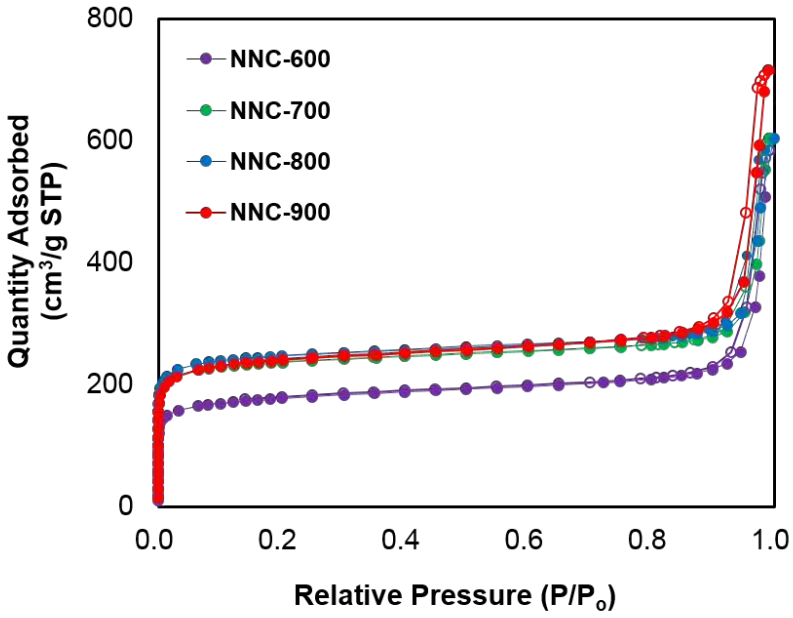

Figure S6: Nitrogen adsorption/desorption isotherm curves of the ZIF-8-derived NNC-X materials; X refers to carbonization temperatures.

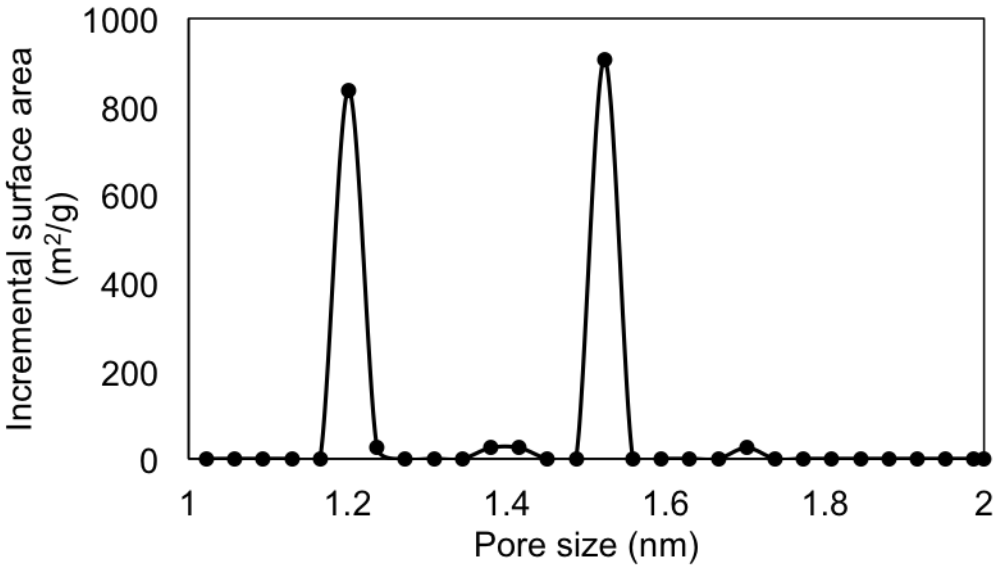

Figure S7: Pore size distribution of the synthesized ZIF-8 material.

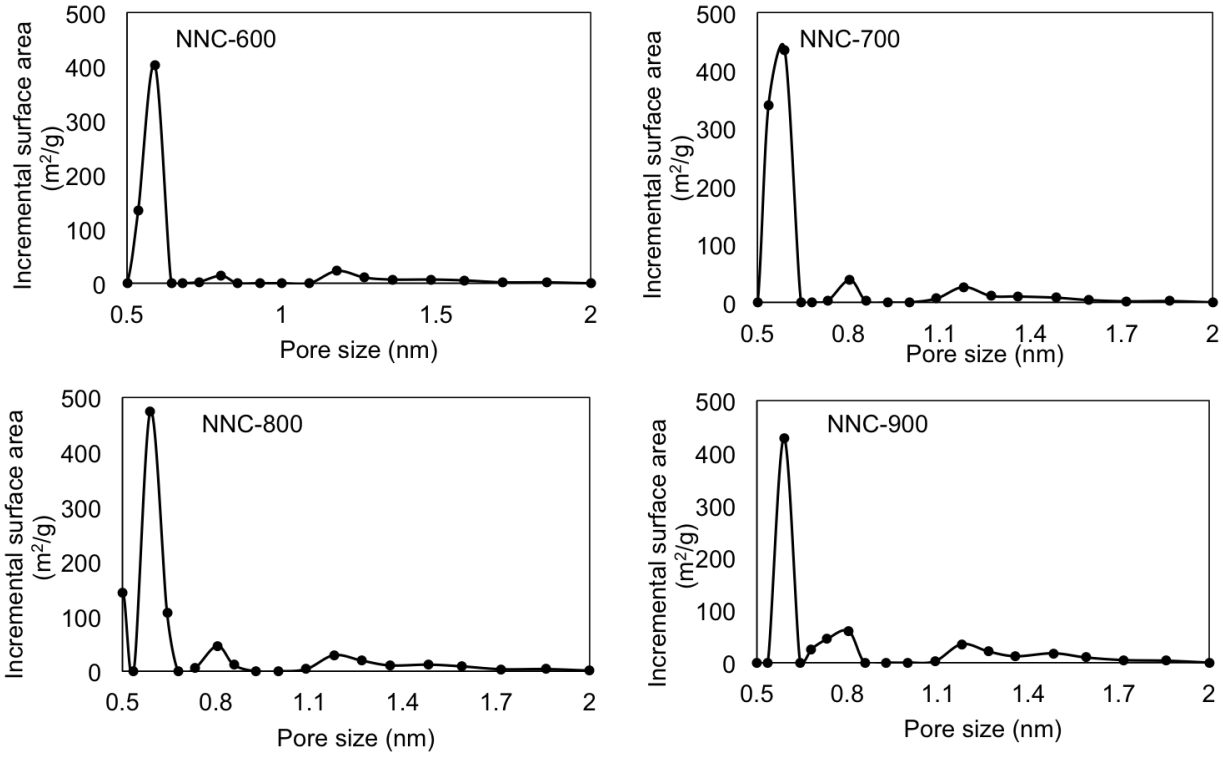

Figure S8: Pore size distributions of the ZIF-8-derived NNC-X materials; X refers to carbonization temperatures.

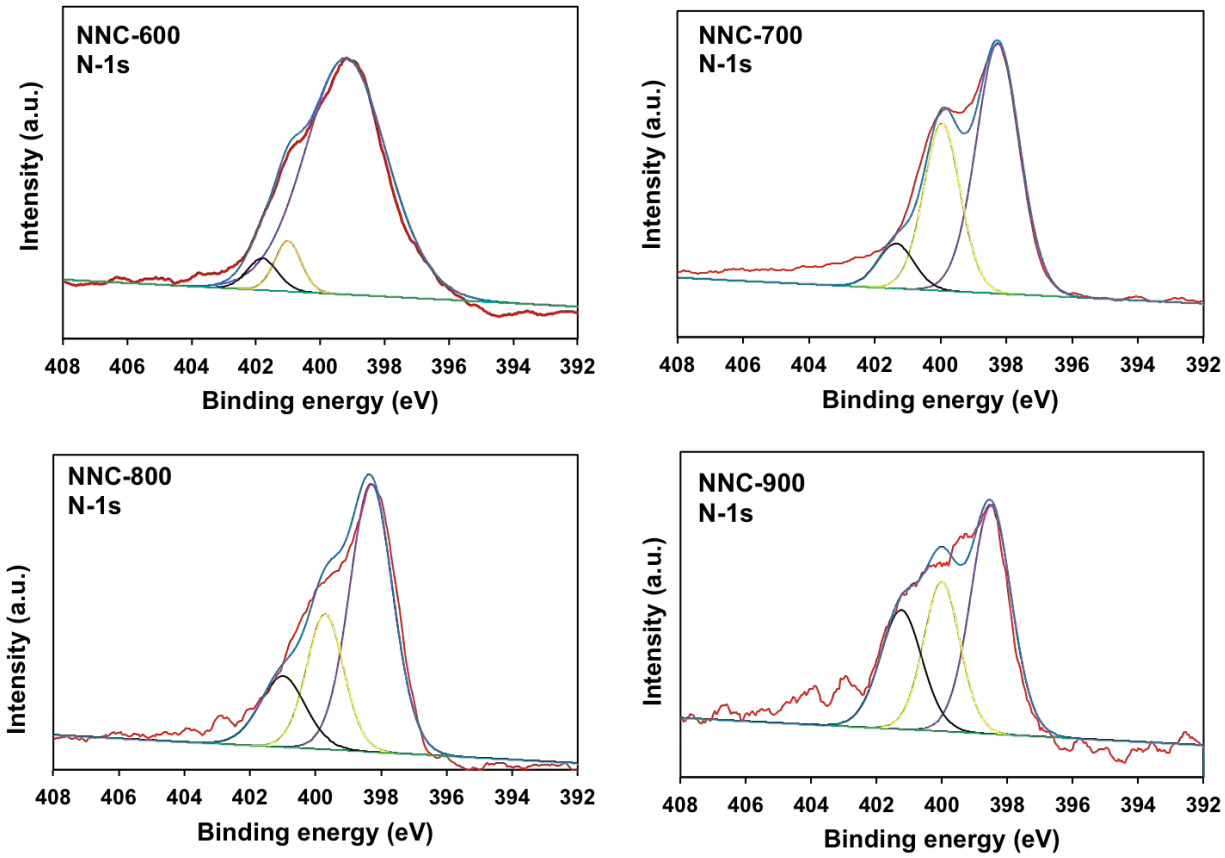

Figure S9: XPS spectra of the ZIF-8-derived NNC-X materials; X refers to carbonization temperatures.

Table S3:The major products of HMF oxidation using different catalysts

Entry	Catalysts	Conversions (%)	Yield of products (%)			
			FDCA	FFCA	HMFCA	Succinic acid
1	NNC-900	100	80	0	0	0
2	NNC-800	100	72	5	4	0
3	NNC-700	100	35	19	16	0
4	NNC-600	100	4	5	12	0
5	ZIF-8	100	0	0	17	0
6	2-MIM	100	0	0	22	0
7	AC	100	0	0	0	0
8	$Zn(NO_3)_2.6H_2O$	100	0	0	3	0
9	Graphite	100	0	0	6	0
10	ZnO	100	0	0	3	30
11	ZnO [a]	100	0	0	<1	4

Condition: HMF (0.63 mmol) in 10 mL water, molar HMF/K_2CO_3 = 1:3, 100 mL·min^{-1} oxygen, T = 80 °C, time = 48 h, 0.2 g of catalysts; 2-MIM: 2-methylimidazole; AC: activate carbon; [a] 8 wt% of Zn.

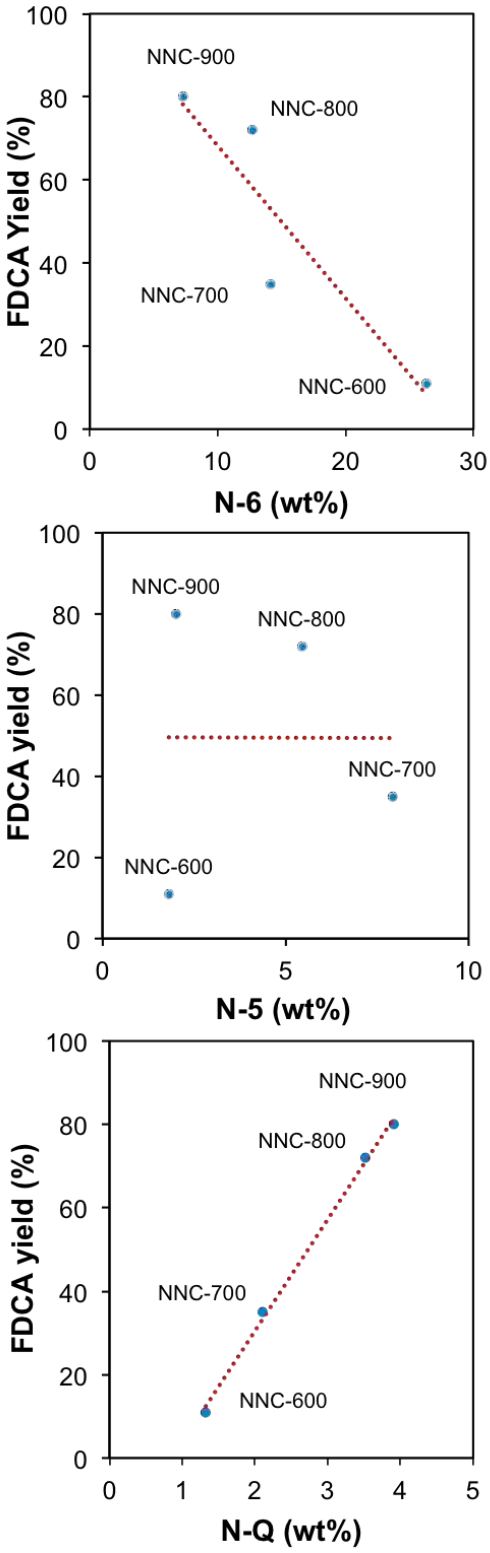

Figure S10: Plotting of the FDCA yield versus three types of nitrogen configuration on NNC-X catalysts.

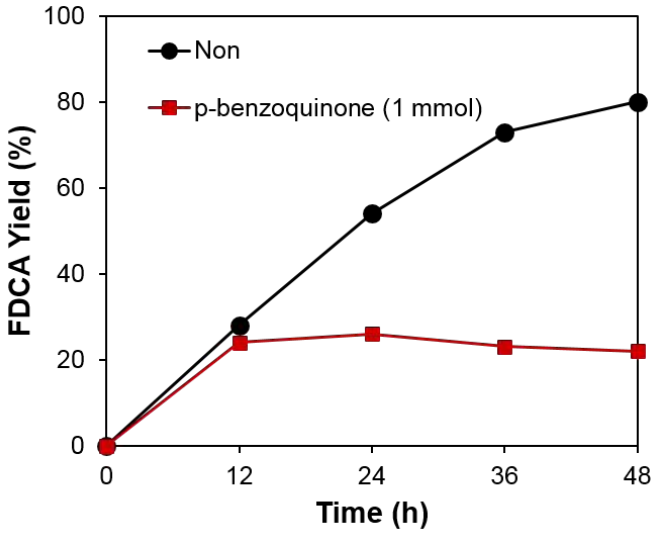

Figure S11: The influence of an anti-radical agent (i.e. p-benzoquinone) on the production of FDCA. Reaction condition: HMF (0.63 mmol) in 10 mL water, 0.2 g NNC-900 catalyst, the molar ratio HMF/K_2CO_3 of 1:3, 100 mL·min^{-1} oxygen gas at ambient pressure.

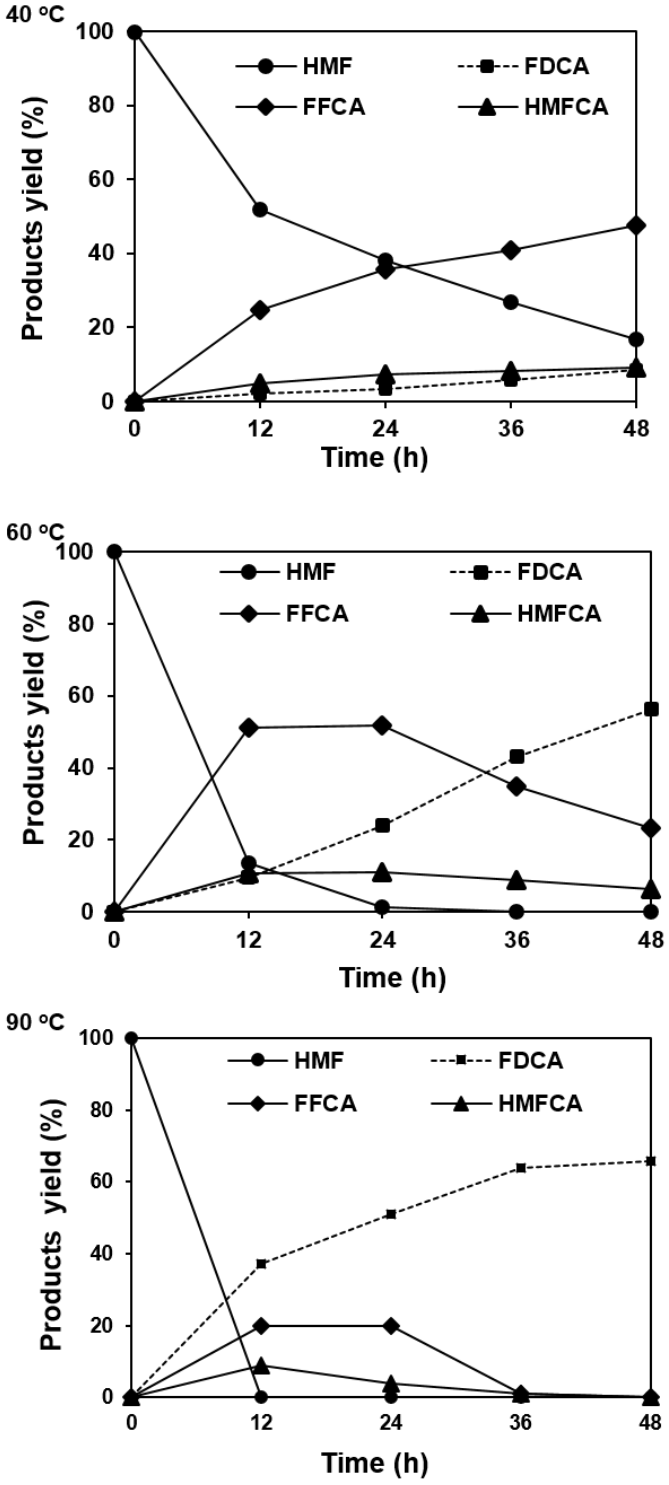

Figure S12: The influence of different temperatures and reaction time on the HMF-to-FDCA conversion. HMF (0.63 mmol) in 10 mL water, 0.2 g NNC-900 catalyst, the molar ratio HMF/K_2CO_3 of 1:3, 100 mL·min^{-1} oxygen gas at ambient pressure.

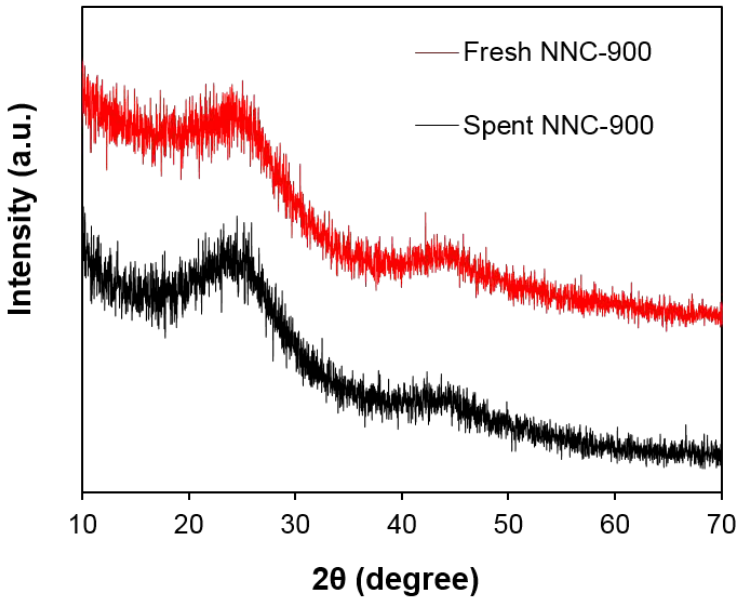

Figure S13: XRD patterns of the NNC-900 catalyst before and after being used in the HMF-to-FDCA conversion.

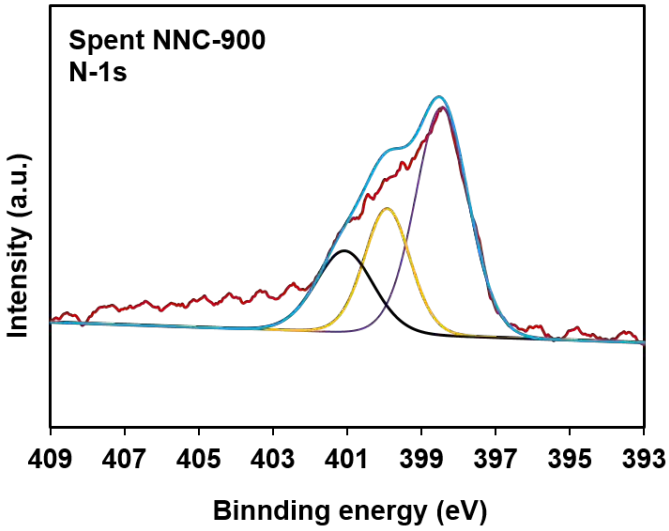

Figure S14: XPS spectra of spent NNC-900 catalyst.

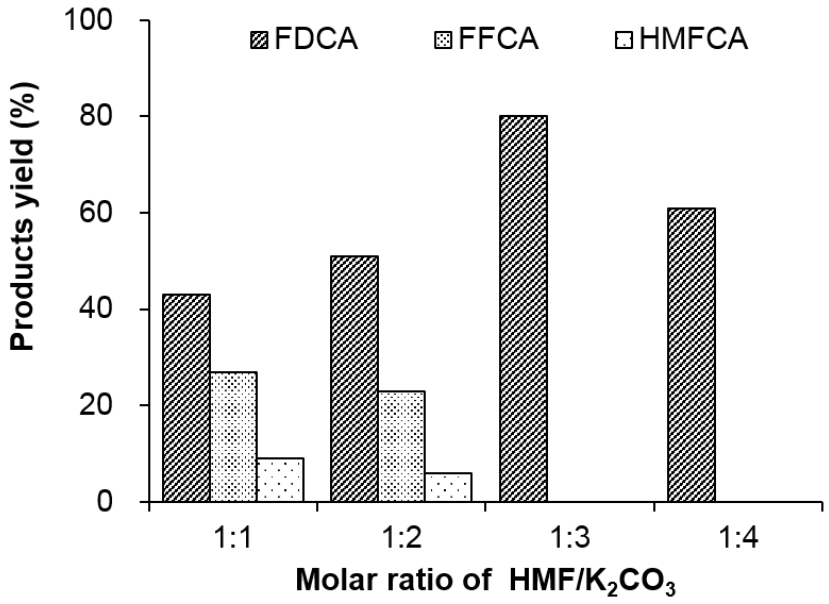

Figure S15: Influence of the molar HMF/K_2CO_3 ratios on HMF-to-FDCA conversion; HMF (0.63 mmol) in 10 mL water, 0.2 g NNC-900 catalyst, the molar ratio HMF/K_2CO_3 of 1:3, 100 mL·min^{-1} oxygen gas at ambient pressure

Table S4: Summation of HMF oxidation via different catalysts

Entry	Catalyst	oxidant	Base	T (°C)	Time (h)	HMF conversion (%)	FDCA yield (%)	Ref.
1	Pt/C	1 bar O_2	1.25M NaOH	25	2	100	81	2
2	Pt/C	1 bar O_2	1 equiv of Na_2CO_3	75	12	100	89	3
3	Pt/PVP	1 bar O_2	No base	80	24	100	94	4
4	Pd/C	690 kpa O_2	2 equiv of NaOH	23	6	100	71	5
5	Pd/C@Fe_3O_4	1 atm O_2	0.5 equiv of K_2CO_3	80	6	98.4	86.7	6
6	Pd/ZrO_2/La_2O_3	1 atm O_2	1.25 equiv of NaOH	90	6	100	90	7
7	Au/CeO_2	0.3 atm O_2	5 equiv of NaOH	60	6	100	73	8
8	Au/HT	1 atm O_2	No base	95	7	99	99	9
9	Au−Pd/CNT	5 bar O_2	No base	100	12	100	94	10
10	Au/TiO_2	20 bar O_2	20 equiv of NaOH	30	18	100	71	11
11	Metal-free (N-doped carbon)	1 atm O_2	3 equiv of K_2CO_3	80	48	100	80	This work

References:

1 F. Zheng, Y. Yang and Q. Chen, *Nat. Comm.*, 2014, **5**, 5261.
2 P. Verdeguer, N. Merat, Gaset, *A.J. Mol. Catal*., 1993, **85**, 327-344.
3 R. Sahu, P. L. Dhepe, *React. Kinet. Mech. Catal.,* 2014, **112**, 173-187.
4 S. Siankevich, G. Savoglidis, Z. Fei, G. Laurenczy, D. T. L. Alexander, N. Yan, P. J. Dyson, *J. Catal., 2*014, **315**, 67-74.
5 S. E. Davis, L. R. Houk, E. C. Tamargo, A. K. Datye, R. J. Davis, *Catal. Today*, 2011, **160**, 55-60.
6 N. Mei, B. Liu, J. Zheng, Kangle Lv, D. G Tang, Z. Zhang, *Catal. Sci. Technol.* 2015, **5**, 3194-3202.
7 B. Siyo, M. Schneider, J. Radnik, M. M. Pohl, P. Langer, N. Steinfeldt, *Appl. Catal. A,* 2014, **478**, 107-116.
8 O. Casanova, S, Iborra, A. Corma, *ChemSusChem*, 2009, **2**, 1138-1144.
9 N. K Gupta, S. Nishimura, A. Takagaki, K. Ebitani, *Green Chem.*, 2011, **13**, 824-827.
10 X. Y. Wan, C. M. Zhou, J. S. Chen, W.P. Deng, Q. H. Zhang, Y. H. Yang, Y. Wang, *ACS Catal.*, 2014, **4**, 2175-2185.
11 Y. Y. Gorbanev, S. K. Klitgaard, J. M. Woodley, C. H. Christensen, A. Riisager, *ChemSusChem*, 2009, **2**, 672-675